SP2 Report on

Reactions of CAC in the Field

Hydration, Conversion, Carbonation and Corrosion

Part 1: Thermal Analysis

Author and Chief Investigator: M. Valix

Summary

- Reduction in surface pH from 12-13 to 8-9 confirm the growth and metabolism of biogenic acid on the surface of the CAC sample.
- Conversion profile was observed with greater conversion being attained at the sewer front and became progressively less close to the concrete substrate.
- Conversion in the 6 year CAC samples has progressed further than conversion attained by curing the CAC at 100°C for 2 hours.
- The extent of conversion in the first half of the CAC specimen (0-2 cm) is about 70-80% and the next half (2-4 cm) is about 35-70%. The CAC cured at 100 °C for 2 hours had a conversion of 46%.
- Corrosion appears to selectively remove C_3AH_6 followed by AH_3. Almost all the C_3AH_6 have been removed in the first 0-2 cm of the CAC specimen from the roof and wall (1500 mm from the sewage floor) and further removal beyond this. The removal of C_3AH_6 is less in the tidal zone. This was attributed to promotion of biogenic acid on the wall and its neutralisation by the alkaline sewage in the tidal zone.
- The rate determining step in the conversion appear to be the conversion of C_2AH_8. This is evident from the higher quantities of C_2AH_8 in comparison to CAH_{10}.

1.0 Introduction

This report provides an assessment of a 6 year old calcium aluminate coating (CAC) that was applied in December 2007 and was sampled by coring in September 18 2013. This CAC was applied in SWOOS 2, North Cell, Hayden Place, Banksmeadow. Three types of cores were taken, one from the roof, 1000 mm from the sewage floor (or tidal zone) and 1500 mm from the sewage floor (or wall).

The main purpose of this analysis was to establish the extent of conversion of the CAC across the coating and to determine the effect of location on this conversion. This was conducted by using thermal analysis (TGA), X-ray diffraction and by scanning electron microscopy and EBSD.

2.0 Experimental

2.1 CAC Preparation

CAC cores were prepared by slicing the cores in layers of 1 cm thickness. Parts of each slice was milled for thermal and XRD. The remaining parts, were examined by SEM and by porosity analysis.

2.2 Characterisation of CAC specimen

The phase transformations during the curing and conversion of CAC were monitored with X-ray diffraction analysis using XRD Siemens D5000 and by thermal gravimetric analysis using Perkin Elmer TGA 4000. Thermal analysis was carried out by heating the samples from 30 to 1000°C with a heating rate of 10°C/min in nitrogen metered at 20 ml/min. The microstructure and mineralogy of selected specimens were examined by scanning electron microscopy using Zeiss ULTRA *plus* with Oxford Instruments Aztec integrated EDS and EBSD system. The surface pH of the cores were determined using a surface pH probe.

3.0 Results

3.1 Surface pH and specimen thickness

The coating thickness are around 4 cm. Measured pH once the samples arrived in our laboratory is around 7-9, although the pH measured in the field suggest the surface pH is closer to 2.0. This could have resulted from the nuetralisation of the surface by the remaining alkaline CAC phase. Nonetheless, the typical surface pH of CAC is 12-13 and the reduction in pH after 6 years demonstrate the microbial activity and the generation of biogenic acid on the CAC surface.

Table 1. Surface pH and thickness of CAC specimen

Core Location	Thickness (mm)					Surface pH				
	1	2	3	Average	Std dev	1	2	3	Average	Std dev
Roof	33.58	49.58	40.02	**41.06**	8.05	8.95	8.9	9.06	**8.97**	0.08
1000mm (tidal zone)	31.89	42.34	40.51	**38.25**	5.58	8.33	7.95	8.2	**8.16**	0.19
1500mm (wall)	52.34	31.12	44.78	**42.75**	10.76	7.26	7.16	7.1	**7.17**	0.08

3.2 Thermal Analysis

3.2.1 CAC Hydrates

Calcium aluminate once hydrated undergoes a series of chemical reaction that influences both its physical, mechanical and chemical properties. The designations for the chemical formulae are C - CaO, A – Al_2O_3, H - H_2O, S – SiO_2, c – CO_2 and C - Ca.

Calcium aluminate cement reacts with water to form metastable (CAH_{10} and C_2AH_8) and stable hydrates (C_3AH_6) through time and temperature dependent reactions (Scrivener, Cabiron et al. 1999, Chotard, Gimet-Breart et al. 2001, Juenger, Winnefeld et al. 2011):

$$CA + 10H \rightarrow CAH_{10} \qquad (T<15°C) \qquad (1)$$

$$2CA + 11H \rightarrow C_2AH_8 + AH_3 \qquad (15°C \ <T<70°C) \qquad (2)$$

$$3CA + 12H \rightarrow C_3AH_6 + 2AH_3 \qquad (T>70°C) \qquad (3)$$

Once hydrated CAC is subjected to further chemical change referred to as conversion that further transform the metastable phases to the stable phase (Bradbury, Callaway et al. 1976):

$$3CAH_{10} \rightarrow C_3AH_6 + 3\,AH_3 + 18H \qquad (4)$$

$$3C_2AH_8 \rightarrow 2C_3AH_6 + AH_3 + 9H \qquad (5)$$

In the presence of pozzolanic vitreous silica or supplementary cementitious materials, it has been suggested that the silica would react with the CA phase to form stratlingite (C_2ASH_8) avoiding the formation of C_2AH_8 and thus the conversion to C_3AH_6 the formation(Hidalgo, Garcia et al. 2009).

$$2CA + S + 11H \rightarrow C_2ASH_8 + AH_3 \qquad (6)$$

The stable phase C_3AH_6 can also react with CO_2 in the atmosphere to form $CaCO_3$ (Cc) (Blenkinsop, Currell et al. 1985):

$$C_3AH_6 + 3c \rightarrow 3\,Cc + AH_3 + 3H \qquad (7)$$

The CAC hydrates were identified according to Table 1. The differential thermal gravimetric analysis (DTG) of CAC obtained from the tidal, wall and roof are shown in Figures 1-3 respectively.

The DTGs of the 6 year CAC specimen are compared with the DTG of a control sample cured for 28 days at 30°C and CAC cured for 2 hours at 100°C. It is apparent that compared to the control CAC, the progression of conversion in CAC after 6 years appear substantial. When compared with CAC cured at 100°C, the extent of conversion after 6 years is also substantial. These are evident from the reduction in the metastable peaks between 100-200°C and both the rise in C_3AH_6 at 310-350°C and AH_3 at 270-290°C. The quantities of the CAC hydrates varied across the coating and these variation is attributed to the effects of hydration, conversion and corrosion. In the tidal zone sample, it appears there is very little of the C_3AH_6 phase that is loss. However in the wall sample (Figure 2) and roof sample (Figure 3), the greater loss of C_3AH_6 closest to the sewer front demonstrate the greater corrosivity of this phase.

Table 1. Thermal decomposition of calcium aluminate hydrates.

Calcium Aluminate Hydrates								Heating Rate	Method	References
CAH_{10}	C_2AH_8	C_3AH_6	AH_3 gel	$Al(OH)_3$	C_2ASH_8	$CaCO_3$	$C_3AH_{1.5}$			
	110, 175, 295							10°C/min	DTG	(Ukrainczyk, Matusinovic et al. 2007)
96				266				20°C/min	DTG	(Barnes and Baxter 1978)
110				267				5°C/min	DTG	(Guirado, Gali et al. 1998)
170	230, 275	320						10°C/min	DTG	(Das, Mitra et al. 1996)
110-120	200	320-350		295-310				25°C/min	DTA	(Bradbury, Callaway et al. 1976)
120		310		290				10°C/min	DTA	(Nilforoushan and Talebian 2007)
			90					10°C/min	DTA	(Calvo, Alonso et al. 2013)
137	137		87	220-280	280-350			10°C/min	DTA	(Hidalgo, Garcia et al. 2009)
					100, 138 and 240			10°C/min	DTG	(Kuzel 1976)
					120, 165 and 220			10°C/min	DTG	(Matschei, Lothenbach et al. 2007)
						700				(Grounds, Midgley et al. 1985)
						>650	550			(Palou, Bagel et al. 2013)

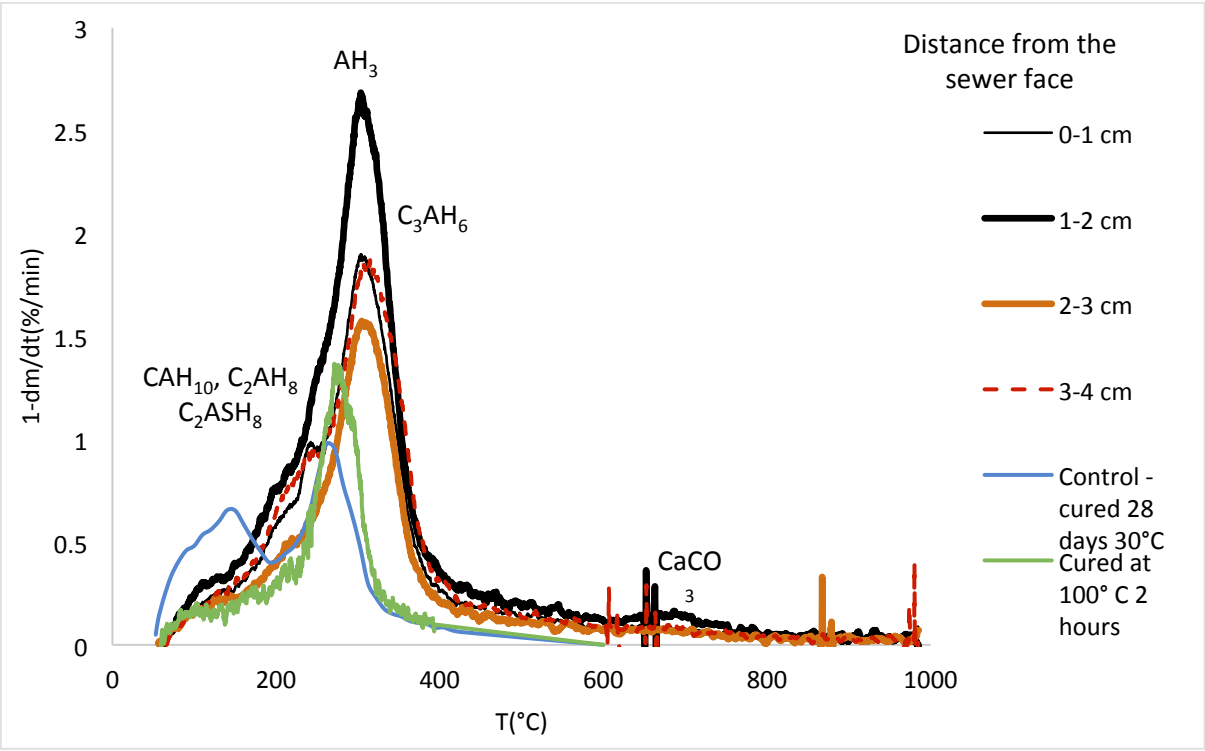

Figure 1. DTG profile of CAC taken from 1000 mm above the sewage floor (tidal zone)

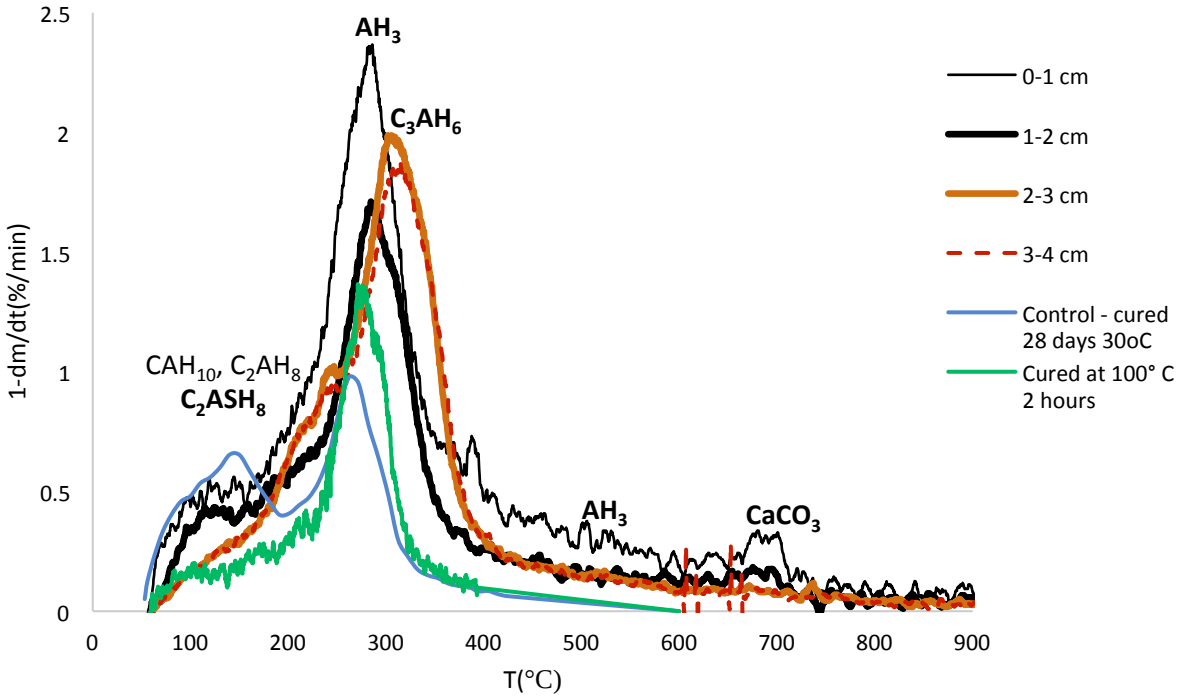

Figure 2. DTG profile of CAC taken from 1500 mm above the sewage floor (wall).

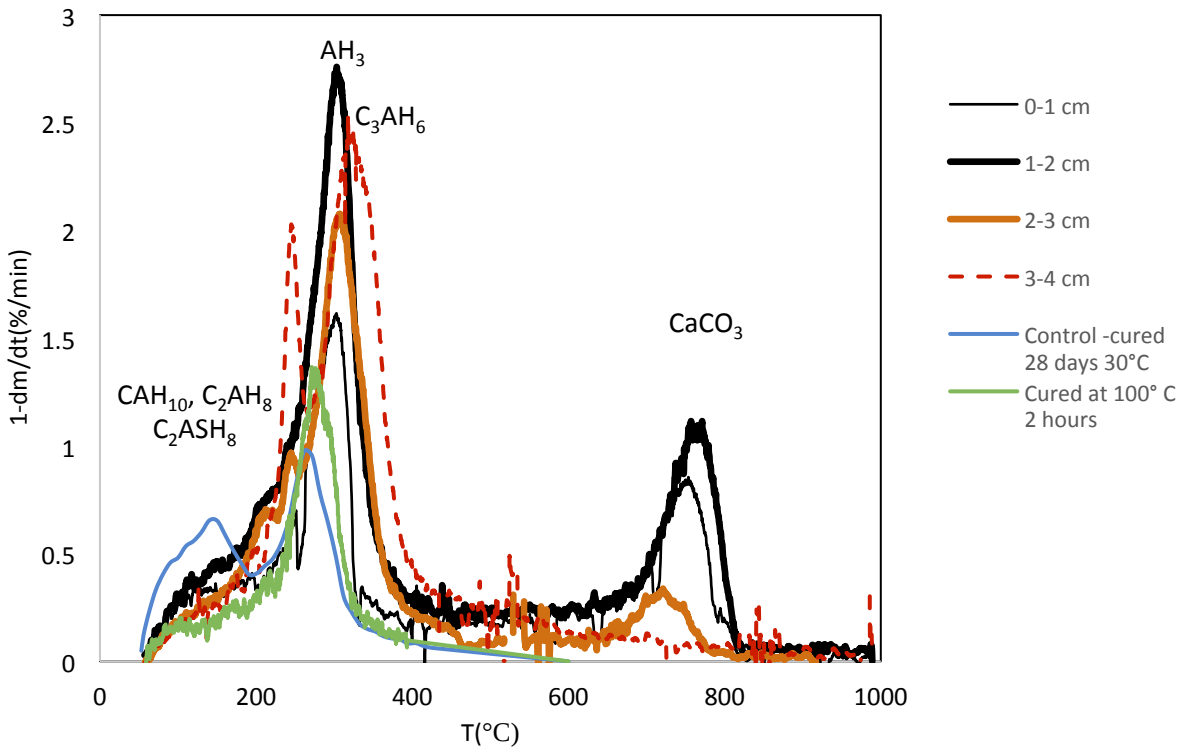

Figure 3. DTG profile of CAC taken from the roof.

CAC was also subjected to the carbonation reaction and this is apparent from the formation of $CaCO_3$ around 600-800°C. Carbonation affected all the samples principally on the top layers closest to the sewer face. Its effect on the tidal zone and wall samples were not significant, whilst its effect on the roof sample was noticeable and appear only the remaining 1 cm layer closest to the concrete substrate was unaffected by carbonation.

3.2.2 Hydration, Corrosion and Conversion Profiles

To examine the hydrated phases on the corroded CAC, the unresolved multi-component bands associated with the individual converted component peaks were separated by using a curve resolving algorithm, based on the Levenberg-Marquardt method (Marquardt 1963). The peak function was a mixed Gauss-Lorentz line shape of the form:

$$\boldsymbol{f(x) = (1-L)He^{-\left[\left(\frac{x-x_0}{w}\right)^2 4ln2\right]} + \frac{LH}{4\left(\frac{x-x_0}{w}\right)^2+1}} \qquad (8)$$

where x_0) peak position; H) peak height; w) peak width; L) fraction of Lorentz character. Figure 12 shows an example of curve fitting analysis of a DTG data.

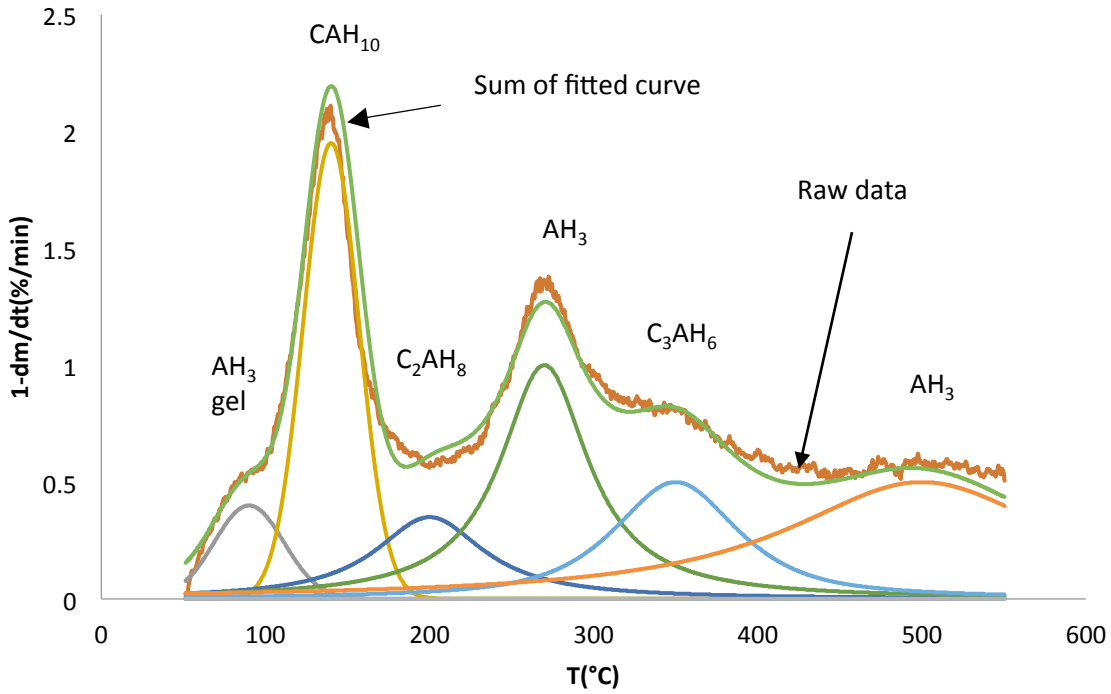

Figure 4. Curve fitting analysis of CAC coupon installed in Sydney North Barrel for 24 months.

The quantities of the metastable phases (CAH_{10} and C_2AH_8) are likely to be subjected by the their formation by the hydration of calcium aluminate (CA) and removal by their conversion to the stable phase. The net effect of these reactions are show in Figures 5 and 6 respectively. The amount of CAH_{10} progressively decreased from the sewer front towards the concrete substrate. This was balanced by counter increase in C_2AH_8.

It has been suggested that the progression of conversion occurs through C_2AH_8 as an intermediate phase(Rashid, Barnes et al. 1994)**:**

$$CAH10 \rightarrow \alpha\, C_2AH_8 \rightarrow \beta C_2AH_8 \rightarrow C_3AH_6 \qquad (9)$$

This suggests that the low CAH_{10} closest to the substrate means most of this phase has been converted to C_2AH_8 according to equation (9). However because C_2AH_8 closest to the concrete substrate remained high its subsequent conversion to C_3AH_6 must have been slower. Whilst CAC closer to the sewer front showed slower CAH_{10} conversion but faster conversion of C_2AH_8. This is evident in the lower areas of C_2AH_8 and higher AH_3 in Figure 7. The amount of AH_3 generated reflects the extent of conversion. In general it appear the rate determining step in overall rate of conversion of CAC appear to depend on the conversion of C_2AH_8 and this is faster closer to the sewer front progressively decreasing close to the substrate.

The relative difference in the metastable phases based on the various location of CAC is also noticeable. It is apparent that the wall has the least amount of CAH_{10} and C_2AH_8. Figure 7 shows the amount of AH_3 generated is also lower relative to the roof and tidal zone. This suggests these lower metastable phases are attributed to the lower hydration reaction in the

wall. Whereas the higher metastable phases and AH_3 in the roof and tidal zone suggests greater hydration and proportionately equivalent conversion reactions at these locations.

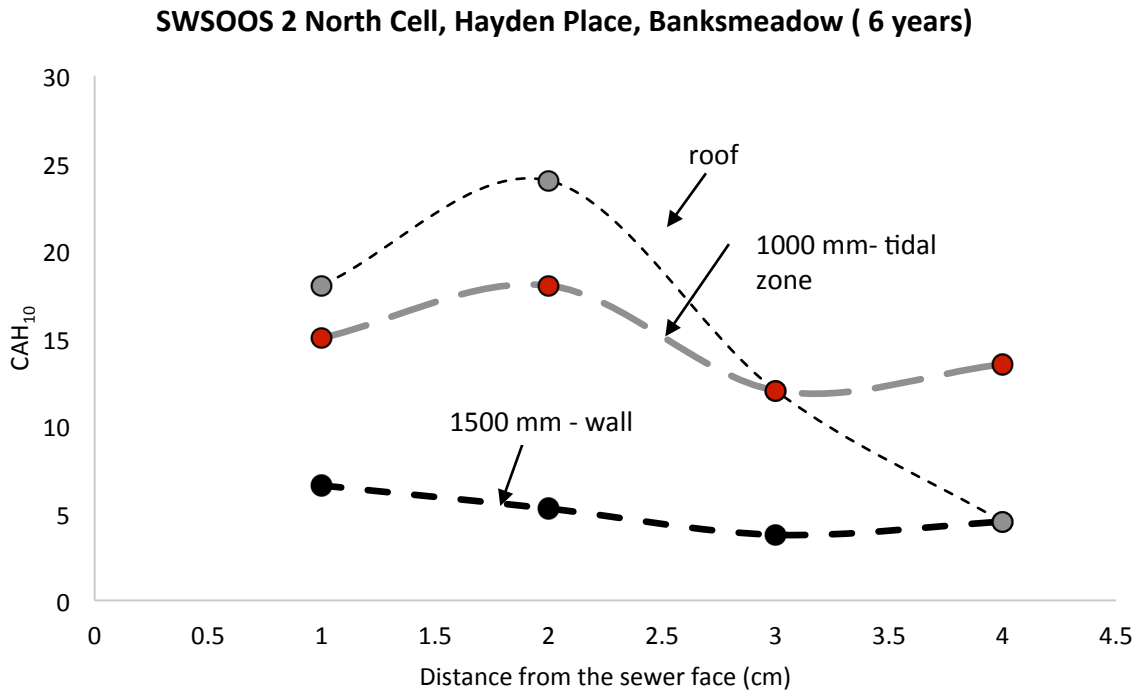

Figure 5. Distribution profile of CAH_{10} across CAC.

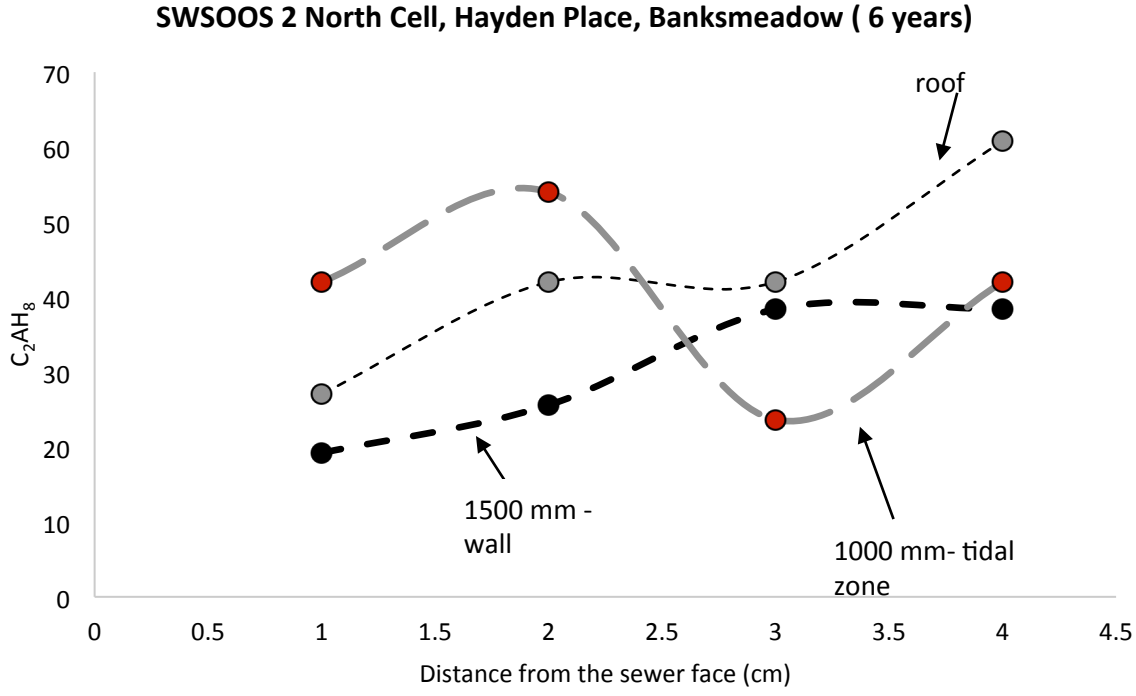

Figure 6. Distribution profile of C_2AH_8 across CAC.

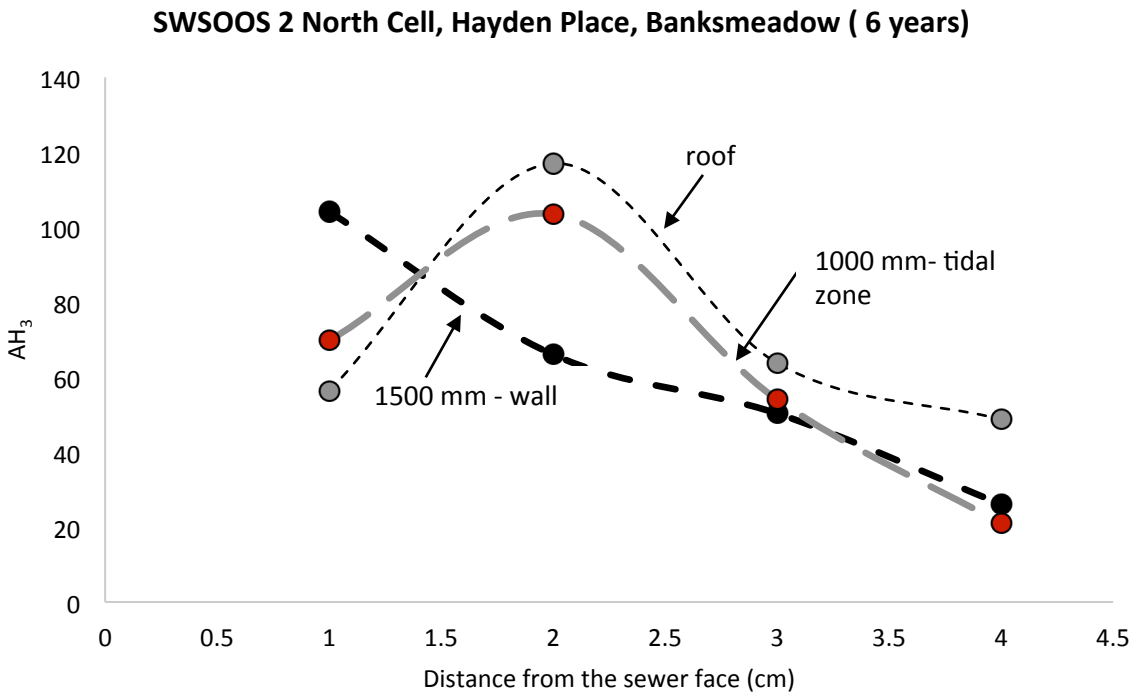

Figure 7. Distribution profile of AH_3 across CAC.

Figure 7 shows also the loss of AH_3 at the sewer front of the roof and tidal samples. Greater amounts of this gibbsite phase are removed in the roof and tidal zone in comparison to the wall.

As shown in Figure 1-3, there is a definite loss of C_3AH_6 from the various DTG peaks closest to the sewer front. A plot of C_3AH_6 profile in Figure 8 shows the corrosion effect more clearly. As shown greater loss of C_3AH_6 was observed at the sewer front, progressively decreasing with CAC samples close to the concrete. The loss is more extensive in the roof and wall, and is significantly less in the tidal zone. This could be attributed to the biogenic acid formation promoted on the walls, whereas the corrosion effect may be neutralised by the alkaline nature of the sewage near the tidal zone.

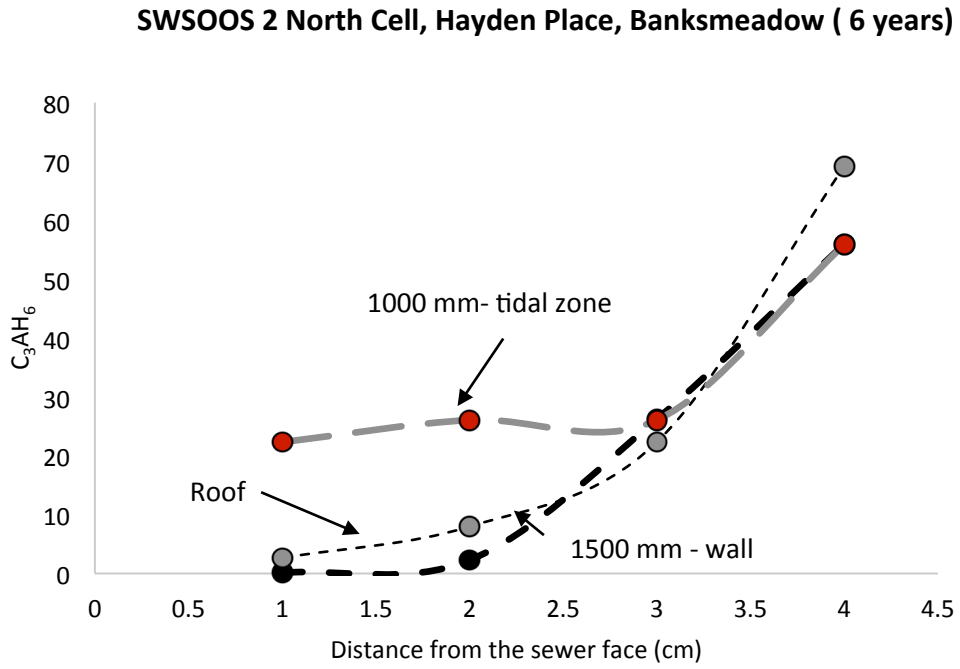

Figure 8. Distribution profile of C_3AH_6 across CAC.

An approximate conversion across the CAC profile as estimated using the following equation:

$$Conversion = \frac{AH_3}{AH_3+C_2AH_8+C_3AH_6} \quad (10)$$

Because the sewer front of the CAC specimens are subjected to corrosion, which includes the removal of AH_3, the conversion estimated at this region may be less than what is experienced by the sample. In the roof and tidal samples, where there is significant removal of AH_3, the conversion were excluded. The estimated conversion profiles are shown in Figure 9. As shown the conversion at the sewer front is greater than close to the substrate. The conversion close to the substrate is very similar to the conversion at the beginning of the installation, which suggest very little progression in conversion has occurred here. The conversion at the beginning of the installation was estimated from a control sample that was cured for 48 hours at 21°C. This observed conversion profile is consistent with the observed trends in the metastable profiles observed in Figure 5 and 6. The extent of conversion in first half of the CAC sample is between 70-80% and the remaining half is from 35-70%. This suggests these first half would be subjected to greater rate of corrosion. The greater loss of C_3AH_6 and AH_3 in this first half (see Figure 7 and 8) confirms this. The location does not appear to affect the conversion.

This conversion profile also places the corrosion of C_3AH_6 in greater perspective. Because the conversion is least closest to the substrate, the C_3AH_6 at this position should also be the

least. However as shown in Figure 8, the C_3AH_6 are all significantly lower above this position, demonstrating the extent of C_3AH_6 corrosion. It should be noted that part of the roof C_3AH_6 have also been converted to $CaCO_3$.

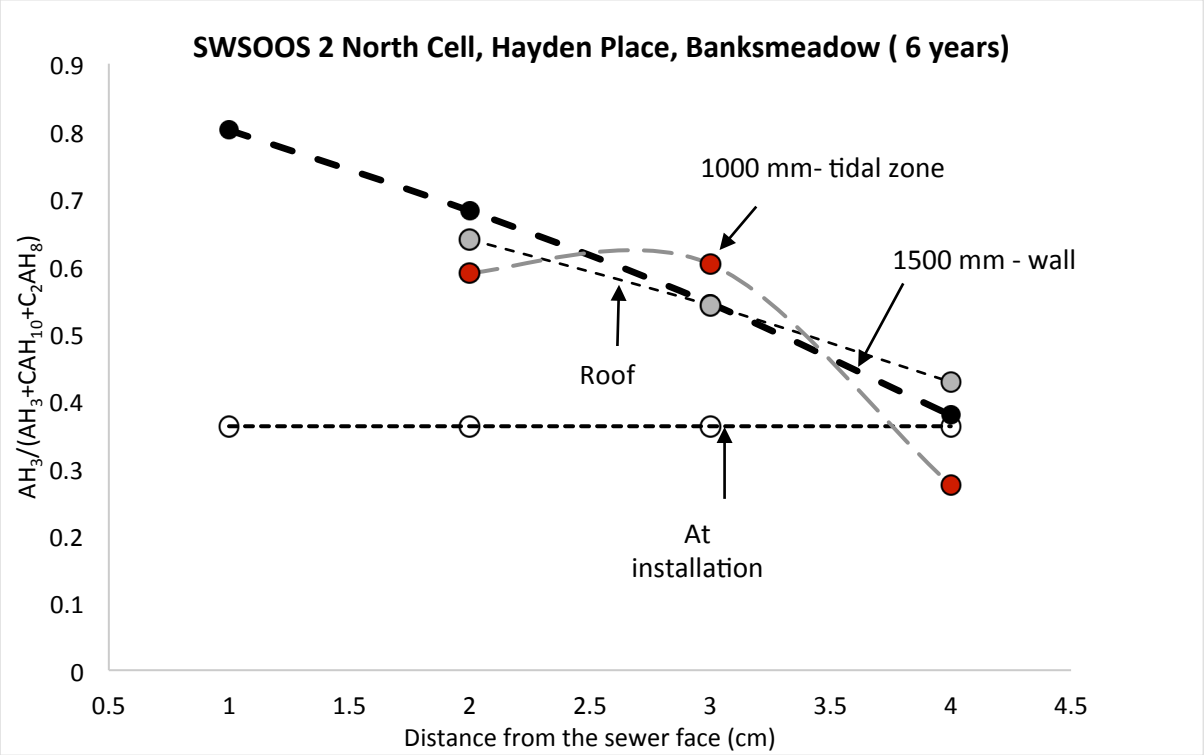

Figure 9. Distribution profile of conversion across CAC.

References

1. Barnes, P. A. and J. H. Baxter (1978). "CRITICAL ANALYSIS OF APPLICATION OF DERIVATIVE THERMOGRAVIMETRY TO DETERMINATION OF DEGREE OF CONVERSION OF HIGH ALUMINA CEMENT." Thermochimica Acta **24**(2): 427-431.
2. Blenkinsop, R. D., B. R. Currell, H. G. Midgley and J. R. Parsonage (1985). "THE CARBONATION OF HIGH ALUMINA CEMENT .1." Cement and Concrete Research **15**(2): 276-284.
3. Bradbury, C., P. M. Callaway and D. D. Double (1976). "CONVERSION OF HIGH ALUMINA CEMENT-CONCRETE." Materials Science and Engineering **23**(1): 43-53.
4. Calvo, J. L. G., M. C. Alonso, A. Hidalgo, L. F. Luco and V. Flor-Laguna (2013). "Development of low-pH cementitious materials based on CAC for HLW repositories: Long-term hydration and resistance against groundwater aggression." Cement and Concrete Research **51**: 67-77.

5. Chotard, T., N. Gimet-Breart, A. Smith, D. Fargeot, J. P. Bonnet and C. Gault (2001). "Application of ultrasonic testing to describe the hydration of calcium aluminate cement at the early age." Cement and Concrete Research **31**(3): 405-412.
6. Das, S. K., A. Mitra and P. K. DasPoddar (1996). "Thermal analysis of hydrated calcium aluminates." Journal of Thermal Analysis **47**(3): 765-774.
7. Grounds, T., H. G. Midgley and D. V. Nowell (1985). "THE USE OF THERMAL METHODS TO ESTIMATE THE STATE OF HYDRATION OF CALCIUMTRISULFOALUMINATE HYDRATE 3CAO.AL2O3.3CASO4.NH2O." Thermochimica Acta **85**(APR): 215-218.
8. Guirado, F., S. Gali and J. S. Chinchon (1998). "Thermal decomposition of hydrated alumina cement (CAH(10))." Cement and Concrete Research **28**(3): 381-390.
9. Hidalgo, A., J. L. Garcia, M. C. Alonso, L. Fernandez and C. Andrade (2009). "MICROSTRUCTURE DEVELOPMENT IN MIXES OF CALCIUM ALUMINATE CEMENT WITH SILICA FUME OR FLY ASH." Journal of Thermal Analysis and Calorimetry **96**(2): 335-345.
10. Juenger, M. C. G., F. Winnefeld, J. L. Provis and J. H. Ideker (2011). "Advances in alternative cementitious binders." Cement and Concrete Research **41**(12): 1232-1243.
11. Kuzel, H. (1976). "Crystallographic data of synthetic gehlenite hydrate." Neues Jahrbuch fuer Mineralogie, Monatshefte: 319-325.
12. Marquardt, D. W. (1963). "AN ALGORITHM FOR LEAST-SQUARES ESTIMATION OF NONLINEAR PARAMETERS." Journal of the Society for Industrial and Applied Mathematics **11**(2): 431-441.
13. Matschei, T., B. Lothenbach and F. P. Glasser (2007). "Thermodynamic properties of Portland cement hydrates in the system CaO-Al2O3-SiO2-CaSO4-CaCO3-H2O." Cement and Concrete Research **37**(10): 1379-1410.
14. Nilforoushan, M. R. and N. Talebian (2007). "The hydration products of a refractory calcium aluminate cement at intermediate temperatures." Iranian Journal of Chemistry & Chemical Engineering-International English Edition **26**(3): 19-24.
15. Palou, M. T., L. Bagel, V. Zivica, M. Kuliffayova and T. Ifka (2013). "Hydration of high alumina cement-silica fume composite with addition of Portland cement or sodium polyphosphate under hydrothermal treatment." Journal of Thermal Analysis and Calorimetry **113**(1): 385-394.
16. Scrivener, K. L., J. L. Cabiron and R. Letourneux (1999). "High-performance concretes from calcium aluminate cements." Cement and Concrete Research **29**(8): 1215-1223.
17. Ukrainczyk, N., T. Matusinovic, S. Kurajica, B. Zimmermann and J. Sipusic (2007). "Dehydration of a layered double hydroxide - C(2)AH(8)." Thermochimica Acta **464**(1-2): 7-15.